

Relationship between scaling behavior and porosity of plasma-deposited TiO₂ thin films

A. Borrás,¹ A. Yanguas-Gil,¹ A. Barranco,¹ J. Cotrino,^{1,2} and A. R. González-Elipe¹

¹*Instituto de Ciencia de Materiales de Sevilla, CSIC-Universidad Sevilla, Avda. Américo Vespucio 49, 41092 Sevilla, Spain*

²*Departamento de Física Atómica Molecular y Nuclear, Universidad Sevilla, Avda. Reina Mercedes s/n, 41012 Sevilla, Spain*

(Received 14 June 2007; revised manuscript received 11 September 2007; published 4 December 2007)

The growth of TiO₂ thin films prepared by plasma enhanced chemical vapor deposition has been studied by analyzing their roughness with the concepts of the dynamic scaling theory. Differences in the growth and roughness exponents have been found depending on the composition of the plasma by using either O₂ or mixtures Ar+O₂ as plasma gas and titanium isopropoxide as the precursor. The slope of the representations of the film roughness against the deposition time yielded values of the exponent β of 0.45 and 0.32 for, respectively, thin films prepared with plasmas of O₂ or mixtures Ar+O₂. Meanwhile, values of the exponent α of 1.15 and 1.89/0.35 were deduced from the power spectral density representations for the films prepared under these two experimental conditions. These values are congruent with growth processes dominated, respectively, by shadowing or diffusion processes. A columnar microstructure was observed by scanning electron microscopy for the thin films prepared with pure oxygen. Meanwhile, homogeneous films were obtained with mixtures of Ar+O₂. The open porosity of the films was determined by measuring water adsorption-desorption isotherms with a quartz crystal monitor. This analysis showed that in the samples prepared with mixtures of Ar+O₂ the porosity consisted exclusively of micropores ($d < 2$ nm), while in the films prepared with an oxygen plasma there were micro- and meso-pores ($d > 2$ nm). It is concluded that the different growth mechanisms found by just changing the chemistry of the plasma are responsible for the quite distinct microstructures, porosities, and optical properties obtained for the films.

DOI: 10.1103/PhysRevB.76.235303

PACS number(s): 81.15.Aa, 81.15.Gh, 81.10.Bk

I. INTRODUCTION

It is well-known that the porosity and microstructure of thin films are crucial factors that determine many of their final properties.^{1,2} In particular, both the optical constants of films used in optics and their evolution in depth are very much dependent on the thin film microstructure.^{3–8} Most works in literature addressing this question refer to thin films prepared by evaporation, while other procedures such as plasma enhanced chemical vapor deposition (PECVD) have not received similar attention.⁹ This situation contrasts with the fact that through the adjustment of a wide range of experimental parameters (i.e., type of plasma gas, pressure, temperature, etc.) PECVD provides great flexibility to control the microstructure of the thin films.^{10–15} The present paper aims at describing and explaining the reasons why different microstructures and porosities are obtained for TiO₂ thin films prepared by PECVD as a function of the composition of the plasma gas used for the deposition. Studies about the microstructure and porosity of TiO₂ thin films are of importance for the control of their optical properties^{11,12} or their photoactivity when used as photoactive materials.¹¹

On the other hand, in the last years there has been an increasing interest in the analysis of the scaling behavior of the surface roughness and its relationship with the growing mechanisms of the thin films.^{16,17} Based on the so-called dynamic scaling theory (DST), these studies rely on the evolution of the surface roughness with the deposition time and the scale of measurement. The evolution of the roughness (α) and growth (β) exponents deduced from this analysis provides information about the influence of the different surface processes controlling the thin film growth (surface diffusion, surface reactivity, shadowing effects, etc.) and, there-

fore, in the shaping of the surface morphology.^{18–21} Roughness evolution of films prepared by plasma deposition usually behave in an “anomalous” way with regard to the values of roughness and growth exponents (i.e., these exponents do not follow the basic Family-Vicsek relation that holds for a “normal” scaling behavior of surface evolution^{22,23}). As evidenced for SiO₂ and SiO_xCy films prepared by PECVD, a factor that contributes to the appearance of such an “anomalous” behavior in plasma films is the fact that species coming from the plasma may reach the surface under off-diagonal directions.²⁴ In the present work we try to get further insights about the influence of the plasma chemistry on the thin film microstructure and porosity. For this aim, a highly oxidative plasma of oxygen and other O₂+Ar gas mixtures with a high concentration of Ar have been used for deposition of TiO₂ thin films. These two conditions have yielded quite different microstructures and porosities for the films.

Here, the porosity of the films has been assessed by measuring adsorption isotherms of water vapor²⁵ with a quartz crystal monitor. A similar technique based on the ellipsometric analysis of the thin films as a function of the relative humidity has been reported for other types of transparent thin films.^{26–30} The procedure utilized here is more general and could also be used for thin films prepared by sol-gel (e.g., mesoporous films³¹) where the existence of a general procedure for determination of porosity is a clear need.

Finally, to explain the quite different microstructures and porosities of films obtained with O₂ or O₂+Ar plasmas, a correlation is intended between the type of porosity of the films and their roughness evolution analyzed under the premises of the DST and their scaling behavior. In addition, an explanation is set up that relates the different characteristics

of the films with the chemistry of the plasma during their synthesis by PECVD.

This paper is structured as follows: Sec. II describes the experimental conditions used for the deposition and the analysis of the films and Sec. III reports the main experimental results obtained and a discussion of them. Section III is organized into sections, each addressing specific issues as determination of porosity (III A), evolution of roughness with time and scale of measurement (III B), and an assessment about growth mechanisms and thin film porosities depending on the different deposition conditions (III C). In Sec. IV, concluding remarks, a general assessment is drawn about the importance of knowing the growth mechanisms of PECVD thin films to get a precise control of their final microstructure and properties.

II. EXPERIMENT

TiO₂ thin films were prepared at room temperature by PECVD in a plasma reactor with a downstream configuration. The experimental setup, previously described in literature,³² consists of a remote plasma source (SLAN from Plasma consult GmbH, Germany) deposition chamber where the deposition is carried out. The source was operated with a power of 400 W with either pure O₂ or mixtures Ar+O₂ (80% or 90% Ar) as plasma gas. The synthesis of the films was carried out at room temperature. Titanium isopropoxide was used as a titanium precursor. Due to low vapor pressure of this precursor at room temperature, it was placed in a heated stainless steel recipient while oxygen (10% of the total flow of gases) was bubbled through it. Both the bubbling line and the shower-type dispenser used to dose the precursor into the chamber were heated at 373 K to prevent any condensation in the tube walls. Total pressure during deposition was $\sim 4 \times 10^{-3}$ torr either with pure O₂ or Ar+O₂ mixtures as plasma gas. Films were deposited simultaneously on quartz crystal monitor elements and on pieces of silicon and fused silica substrates. The quartz crystal monitor elements were used to measure water adsorption isotherms as described below.

All the films were transparent and their analysis by x-ray photoemission spectroscopy (XPS)/depth profiling only yield as a result a small contamination by carbon (3% to 4%) that was similar in all cases. All the films were amorphous by x-ray diffraction.

The effective refraction index (\mathbf{n}) of the films was determined by UV-vis absorption spectroscopy (Perkin-Elmer Lambda 12 Spectrometer) and by spectroscopic ellipsometry (SOPRA) after the samples have been prepared and exposed to the air. In the former case the refraction index of the films was determined by simulating the oscillations appearing in the spectra of TiO₂ thin films deposited on a substrate with a smaller refraction index. The spectroscopic ellipsometry experiments were performed using a SOPRA commercially available system. The measurements of ellipsometric parameters were made at wavelengths from 0.21 to 1.0 μm at three different angles of incidence, 65°, 70°, and 75°. The reported values of refraction index measured by UV-vis or ellipsometry were determined at $\lambda = 550$ nm. These two techniques

yielded similar values of the refraction index, except for differences of the order of 0.01 in some determinations. These differences will not be considered for the discussion of the results.

Atomic force microscopy (AFM) images were collected in an AFM dimension 3100 from Digital Instrument in tapping mode using high frequency levers. AFM images were processed by WSxM free available software from Nanotec. Roughness of the films, expressed as the root mean square (RMS) value of their surfaces, has been calculated from the images by using this software.

Scanning electron microscopy (SEM) cross section and normal images were measured in a Hitachi S5200 field emission microscope for TiO₂ thin films grown on silicon. Water adsorption-desorption isotherms were measured at room temperature by dosing increasing amounts of water vapor in a chamber where a quartz crystal microbalance (QCM) with the deposited TiO₂ film on its surface was placed. The QCM plates were heated under vacuum at approximately 120 °C by irradiation with a halogen lamp placed in its vicinity. Heating the QCM with the thin films prior to the measurement of the adsorption isotherms was a crucial step for the reproducibility of the results. This was particularly true for some of the examined thin films where water remains adsorbed in its pores at room temperature, even if the samples are maintained in vacuum for long periods of time. Once the samples have been heated and the adsorbed water removed, they were cooled to room temperature and an adsorption isotherm was measured by following the signal of the QCM as a function of the water pressure in the chamber for both the adsorption and desorption cycles of the experiment. To compare the different isotherms, they were corrected by the mass thickness of each thin film. Total pore volume was estimated under the assumption that, once water vapor saturation pressure was reached, the whole pore volume of the films was filled with water. Note that this assumption would not be correct if nonaccessible pores exist in the films.

III. RESULTS AND DISCUSSION

A. Microstructure and porosity of thin films

The deposition rates measured for the TiO₂ thin films were 5 nm min⁻¹ for the O₂ plasma and 3.5 and 2.4 nm min⁻¹ for the Ar+O₂ plasmas containing, respectively, 80% and 90% Ar. The higher growing rate of the samples prepared with the plasma of pure oxygen is likely related with a high concentration of active oxygen species detected in the plasma during these conditions. On the other hand, for the three reported conditions, the measured \mathbf{n} values were 2.05 (plasma of pure O₂) and 1.95 (plasma of 80% and 90% Ar) for films of a thickness $d > 500$ nm.

The deviation of the \mathbf{n} values of the TiO₂ thin films with respect to that of the single crystals of this material ($\mathbf{n} = 2.48$ for the anatase phase³³) should be accounted for by the existence of some empty space in their structure (i.e., porosity). In principle, a microstructure with voids and pores should be visible when examining the samples with SEM. Figure 1 shows SEM micrographs of the thin films prepared with, respectively, a oxygen plasma and another of Ar+O₂

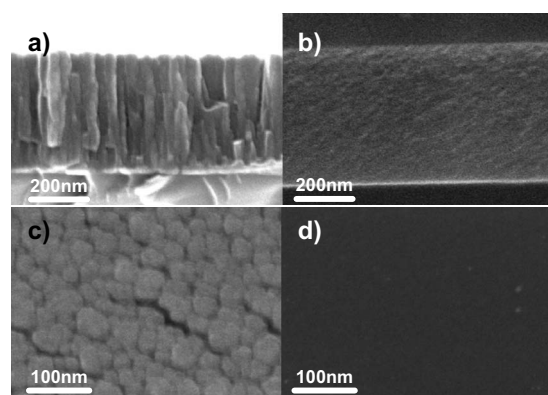


FIG. 1. Cross section [(a) and (b)] and planar views [(c) and (d)] SEM micrographs of the TiO_2 thin films prepared by PECVD with a 100% O_2 [(a) and (c)] and 10% O_2 -90% Ar [(b) and (d)] as plasma gas. Note that the substrate is in the bottom of the view in (a) and (b).

(the microstructure was very similar for 80% and 90% Ar in the plasma gas and no additional comment will be made here to differentiate these two types of samples). In the first case, the micrograph depicts a typical columnar microstructure. This contrasts with the homogeneous microstructure of the sample prepared with the Ar+ O_2 plasma, where no defined defects or pores can be observed in its cross-section image. The absence of pores or columns in this sample might suggest that it is rather compact, in apparent contradiction with the relatively low refraction index of this type of thin films. To clarify this apparent contradiction and to get a precise description of the film porous structure, we have measured water adsorption isotherms for the two types of thin films investigated in this work. The thickness of the investigated films was about $0.5 \mu\text{m}$. The corresponding curves are plotted in Fig. 2 including both the adsorption and desorption branches. The two types of isotherms are quite different. The isotherm corresponding to the samples prepared with Ar+ O_2 plasmas has a type I shape according to the IUPAC classification.²⁵ Type I isotherms are typical of the adsorption in small micropores with a size smaller than 2 nm. An interesting feature is that the desorption branch of this isotherm does not show any significant hysteresis being the adsorption-desorption process completely reversible. By contrast, the isotherm of the O_2 plasma sample presents a shape close to that of type IV of the IUPAC classification. It also presents a strong and irreversibly hysteresis indicating that a considerable amount of water remains in the pores after the completion of the desorption cycle. The irreversibility of this first water adsorption was proved by performing a second adsorption-desorption cycle. The second isotherm performed with this sample is also reported in Fig. 2 (top). It starts at the final position of the desorption branch of the first isotherm and defines a different second cycle. These results prove that outgassing the thin films by heating in vacuum is a crucial step of the experimental protocol that permits one to completely empty their pores prior to the first water adsorption experiment. Note that a sample of this kind exposed to the air would be characterized by an adsorption isotherm with a shape close to that of the second isotherm in Fig. 2

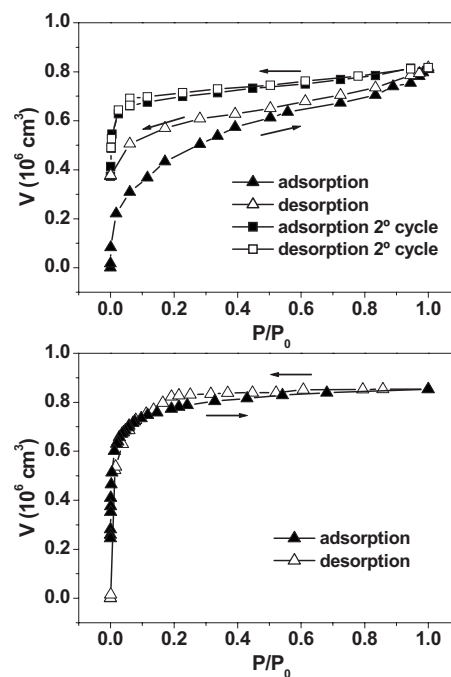


FIG. 2. (top) First and second water isotherms of TiO_2 thin film prepared by PECVD with 100% O_2 . (bottom) Water adsorption and desorption isotherms of TiO_2 thin film prepared by PECVD with 10% O_2 -90% Ar as plasma gas.

(top). This feature of our experimental protocol is not contemplated in similar experiments reported in the literature where heating treatments in vacuum prior to the adsorption experiment are usually missing.²⁶⁻²⁸

The comparison of the adsorption isotherms reported in Fig. 2 for the two samples clearly reveals their different microstructure and sheds some light onto the apparent contradiction between the SEM micrographs and the refractive indices of the films. Thus, although the values of the total porosity, estimated from the values of maximum water adsorption at saturation conditions, are quite similar for the two samples (i.e., around $0.8 \times 10^{-6} \text{ cm}^3$), the different shape of the isotherms suggests that the type, size, and size distribution of pores must be completely different.²⁵ To get a more precise assessment of the pore size distribution in these two thin films we have represented the data of the adsorption branches in the form of a t-plot.²⁵ This type of representation is typical for the analysis of porosity in powder materials and gives an indication of the type and distribution of different pores existing in a sample. For this type of representation we have used the Halsey-Wheeler equation²⁵ assuming an equivalent diameter for the water molecule of 1.3 \AA .³⁴ T-plots permit one to estimate the volume of micro- (pore size smaller than 2 nm), meso- (pore size between 2 and 50 nm), or macro-pores (pore size greater than 50 nm) present in the films.²⁵ The corresponding curves are plotted in Fig. 3. The curve for the sample prepared with Ar+ O_2 plasmas is typical of micropores (pore size $d < 2 \text{ nm}$), without practically any contribution from other types of pores. The micropore volume, determined from the extrapolation of the “plateau” region of the curve is $\sim 0.85 \times 10^{-6} \text{ cm}^3$, in

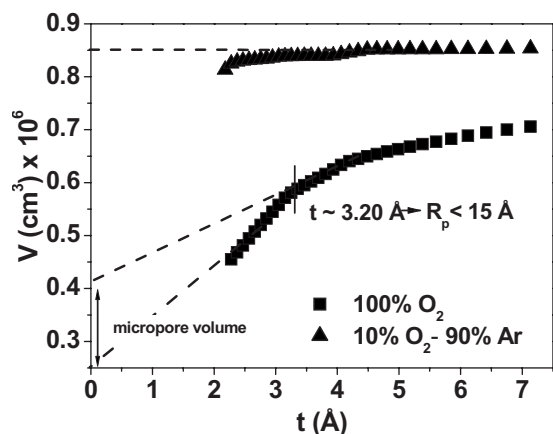


FIG. 3. “t-plots” of the adsorption isotherms for TiO₂ thin films prepared by PECVD with 100% O₂ plasma (first cycle) and 10% O₂-90% Ar plasmas.

good agreement with the total volume of pores deduced from the adsorption isotherm. The t-plot curve of the O₂ sample is more complex resulting from the contribution of both micropores and mesopores. The volume of micropores can be estimated by extrapolation of the dotted-dashed line plotted in Fig. 3.²⁵ In this case, the estimated micropore volume was $\sim 0.40 \times 10^{-6} \text{ cm}^3$. This value accounts for $\sim 50\%$ of the total pore volume (i.e., $0.78 \times 10^{-6} \text{ cm}^3$) of this sample.

B. Analysis of roughness evolution with thickness

The evaluation of the surface roughness as a function of both film thickness and scale of measurement within the frame of the dynamic scaling theory permits one to assess the growth mechanism of the films.¹⁶ Such an approach has been successfully applied for thin films grown by evaporation,¹⁸ sputtering,¹⁹ thermal CVD,³⁵ or PECVD.^{20,21,24} Here, besides applying this methodology, we will try to correlate the obtained information with the porosity and microstructure of the films.

Monitoring the surface roughness by AFM for samples grown for increasing periods of time (i.e., for increasing thickness by assuming that the growth rate is constant) is the most common experimental method used for this type of analysis.¹⁶ Figure 4 shows a set of AFM images for thin films prepared with O₂ and Ar+O₂ plasmas for increasing periods of time and hence increasing thickness. It is already clear from these images that the roughness of the O₂ plasma films is larger than that of the Ar+O₂ plasma films. In addition, it can be qualitatively concluded that for the two series of samples the roughness increases with their thickness.

A more precise evaluation of the roughness of the films can be gained by looking at the line profiles measured on the AFM images. Lines profiles of the AFM images are presented in Fig. 5. A close look to these profiles reveals that for the O₂+Ar samples there are two types of superimposed structures. The first one corresponds to oscillations of approximately 10 nm that seem to coalesce in bigger structures of 70–80 nm as the thickness of the film increases. Meanwhile, in the line profiles of the O₂ plasma samples there is

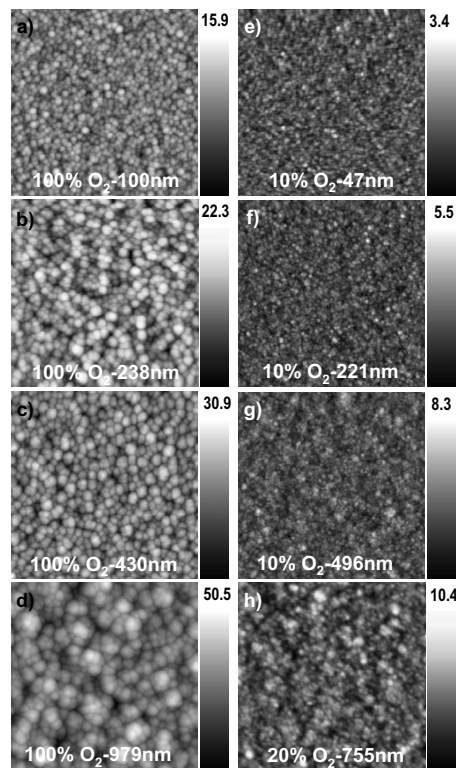


FIG. 4. AFM images of the surface of the TiO₂ thin films with increasing thickness prepared by PECVD with O₂ [left, (a)–(d)] and Ar+O₂ [right, (e)–(h)] as plasma gas. Thicknesses of the films are indicated in the figure. Images of samples with similar thickness prepared with the two plasma gases have been chosen to stress the differences in roughness.

only one type of structure of about 30–40 nm that grows in height with the deposition time.

A way of getting information about the factors that are controlling the microstructure of the thin films during their growth is to plot their roughness, determined from the AFM images, as a function of the deposition time (or their thickness for films prepared for increasing periods of time at constant deposition rate). The corresponding plot for the two types of thin films considered here is shown in Fig. 6 where the roughness of the films (σ) expressed in terms of their rms values has been plotted against their thickness. From this plot it is possible to confirm that the samples synthesized with O₂ plasma are rougher than those prepared with mixtures Ar+O₂. In this later case it is interesting that the data for two gas compositions (i.e., 10% and 20% O₂) depict a quite equivalent tendency. This confirms that their growth mechanism is equivalent for relatively high Ar concentration in the plasma gas.

A significant experimental result is that, for all experimental conditions used, the evolution of surface roughness follows the scaling law $\alpha \sim t^\beta$ (t , thickness of the films is proportional to the time of growth when the deposition rate is constant), which implies a linear dependence between the two magnitudes in the log-log representation used in Fig. 6. Such a dependence is in agreement with one of the assumptions of the DST, with β being the so-called growth expo-

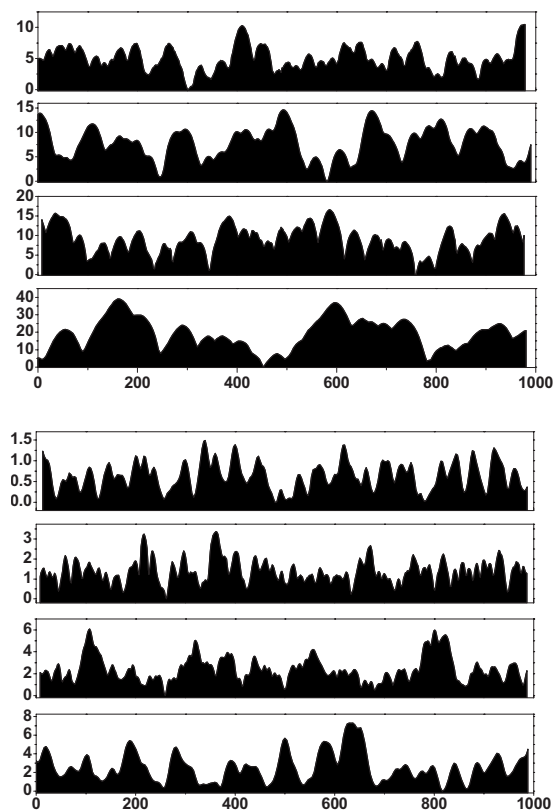


FIG. 5. Line profiles obtained from the AFM images (a)–(d) and (e)–(h) in Fig. 4 for the thin films prepared with O_2 (top) or $Ar+O_2$ (bottom) plasmas. The scale used for the representation of the z axis of each image and plot is different as indicated.

ment. Thus the slope of the representations in Fig. 6 permits one to calculate the growth exponent by adjusting the points to a straight line. For the two series of points represented in Fig. 6, the calculated β values are 0.45 and 0.32, respectively, for the films prepared with plasmas of O_2 or $Ar+O_2$. Note, however, that for the range of thin film thickness investigated here the roughness does not reach saturation. This behavior, contrary to the premises of the Family-Vicsek re-

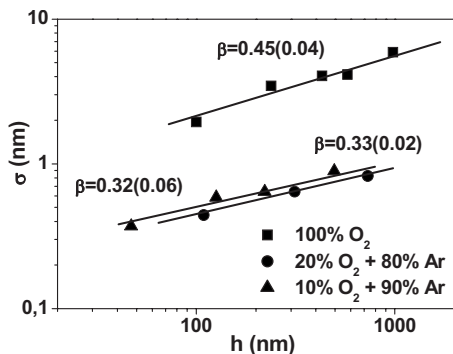


FIG. 6. Representation of the roughness of the films, expressed as rms values, as a function of the thin film thickness (taken as a measurement of the deposition time) for TiO_2 thin films prepared by PECVD with O_2 and $Ar+O_2$ as plasma gas. In this latter case, data for two gas compositions are shown.

lation, may imply either that thicker films should be prepared or an “anomalous” behavior of such thin films.

Within the DST, a number of different theoretical models have been developed in order to explain the values of the scaling exponents, and in particular the growth exponent β .²³ Of these, probably the best known are the random deposition model (i.e., $\beta=0.5$),^{23,35} the so called KPZ model (i.e., $\beta\sim 0.22$)^{23,35,36} or others controlled by diffusion like in MBE deposition (i.e., $\beta\sim 0.2$).³⁷ The experimental β values obtained in our case are relatively close to theoretical values of 0.5 and 0.25/0.20.

Further information about the scaling properties of the films can be obtained from the so-called “power spectral density” of a wave vector [PSD(k)] from the AFM images.^{16,35} This is defined for two-dimensional images as the radial average of the conjugate product of the Fourier transform of the surface and it provides information about the dependence with the scale of measurement of the surface roughness and the self-affine scaling behavior of the films surface.

According to the DST, there exist two regions in which the surface roughness depends on the scale of measurement following two different asymptotic behaviors:¹⁶ below a cut-off length, the roughness changes with the scale of measurement L following the scaling law: $\alpha\sim L^\alpha$ where α is the so-called roughness exponent. That is, below the cutoff length the surface behaves as a self-affine statistic fractal. Over the cutoff length, the surface roughness is constant and invariant with the scale of measurement. As a consequence of this behavior, the PSD is characterized by two different regions: for low correlation lengths ($k\gg$), PSD(k) behaves so that $\log PSD(k)\propto k$, while for high correlation lengths ($k\ll$) the $\log PSD(k)=\text{const}$.

Figure 7 shows the PSD curves deduced from the AFM images of O_2 and $Ar+O_2$ samples with a similar thickness around 500 nm. For the TiO_2 samples prepared with a plasma of pure O_2 , the PSD(k) shows that the α exponent calculated from the slope of the PSD curve before saturation has a value of 1.15. It is also interesting that the saturation of the PSD curve is obtained for correlation lengths around 30–40 nm, a value similar to the average particle size deduced from the linear profiles of this sample [cf. Fig. 5 (top)]. Moreover, this α value is very similar to the value of 1.2 which, associated with relatively high β values, is considered as an “anomalous” situation where the growth is dominated by shadowing effects.³⁴ Thus the PSD curve tells us that for lengths within the particle size as observed by AFM, the roughness is much affected by shadowing effects. Meanwhile, for larger scales of measurements the heights of the interface are uncorrelated. This would support the fact that for this set of samples the growth exponent β is close to 0.5, a value that might indicate a random evolution of the surface features. It is reasonable to associate such a random evolution to a statistically independent growth of the different columns defining the microstructure of the films [cf. Fig. 1(a)]. In favor of this assumption is the fact that the size of the columns is similar to the maximum correlation length found before saturation [cf. Fig. 7 (top)] and to the size of the structures detected in the line profiles of these samples [Fig. 5 (top)].

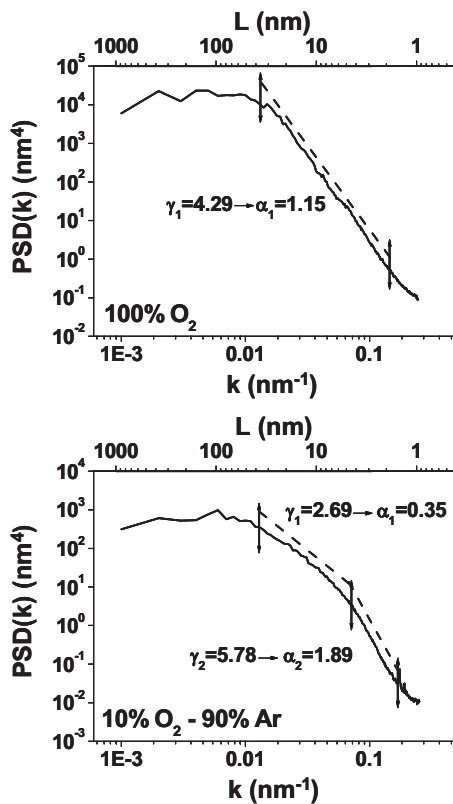


FIG. 7. PSD curves as a function of k deduced from images (b) and (f) of Fig. 4. They correspond to TiO_2 samples prepared with O_2 (top) or mixtures 10% O_2 -90% Ar (bottom) as plasma gas. The length scale is incorporated in the figure in the upper x axis.

On the other hand, the O_2 +Ar sample presents a PSD curve where two different slopes are observed before the curve reaches saturation. At low correlation lengths, the α parameter presents a very large value of 1.89, while for relatively larger correlation lengths this parameter takes a value of 0.35. It is also interesting that the transition from one to the another slope found in this PSD curve occurs for correlation lengths around 5 to 6 nm, of the same order than the average size of the smallest structures present in this sample as deduced from its linear profiles in Fig. 5 (bottom). The highest α value must correspond to the region where the grains are formed, while the smallest value reflects the grain aggregation process in bigger structures. In this sense it must be mentioned that the smallest α value is close to the value of this exponent characteristic of the KPZ scaling equation ($\alpha \sim 0.36$), which accounts for lateral growth and surface relaxation processes.¹⁶ Meanwhile, very high α values ($\alpha \gg 1$), attributed to β values around 0.35, have been associated in literature to anomalous behavior dominated by surface diffusion.^{38,39} It is important to stress that in plasma grown thin films lateral growth can be particularly important because plasma species may arrive to the surface according to off-normal directions.²⁴

C. Growth processes by PECVD and thin film porosity

In literature, growth exponents $\beta \approx 0.45$ and a nonsaturation behavior of roughness with deposition time have been

associated with growth processes characterized by very high sticking probabilities of the fragments (particles) reaching the surface.^{24,35} Typically, such a situation leads to the development of columnar microstructures. The analysis of the PSD curve of the sample prepared with a plasma of 100% O_2 fits within this scheme. We therefore conclude that under these plasma conditions, surface diffusion is restricted or suppressed and the species coming from the plasma remain in the same place where they touch the surface. Shadowing and development of a columnar microstructure is then a likely result.²⁴ This is in fact the situation found for this type of sample where similar-sized columns grow in height up to the surface of the films (cf. Fig. 1).

By contrast, the samples prepared with Ar+ O_2 plasmas are characterized by $\beta \sim 0.32$, a value that suggests that surface diffusion of *ad-species* may be important in controlling the growth of the films. Enhanced diffusion should prevent the appearance of columnar microstructures and favor a granular microstructure instead. At high correlation lengths, this assumption is supported by the value of the α exponent of 0.35 [cf. Fig. 7 (bottom)].

Since the temperature of the substrate (i.e., 298 K) is similar for the two types of thin films a reasonable hypothesis to account for the two types of growing mechanisms is that the plasma species arriving to the surface are different in the two cases. TiO_2 thin films prepared with the plasma of pure O_2 present a relatively high growing rate (i.e., 5 nm min^{-1} against $3.5\text{--}2.4 \text{ nm min}^{-1}$ for the films obtained with Ar+ O_2 plasmas), a fact that points to that this plasma is very efficient in inducing a considerable fragmentation and oxidation of the titanium isopropoxide precursor in the plasma phase. This has been confirmed recently by means of the optical emission spectroscopy (OES) characterization of the plasma, showing the formation of CO^* , CO^+ , CH^* , and TiO^* species.⁴⁰ As previously proposed, highly fragmented titanium species containing Ti-O (Ref. 40) and/or Ti-O-Ti (Ref. 41) structures will bind tightly at the point where they reach the TiO_2 surface. No surface diffusion of *ad-species* is expected under conditions. By contrast, for the films obtained with plasmas rich in Ar, the titanium species coming from the plasma must be neither completely oxidized nor extensively fragmented (i.e., they must consist of fragments of the type TiO_xCy , where part of the 12 carbon atoms of the precursor molecule are still attached to the titanium). This is actually suggested by the fact that the OES spectra recorded under these conditions only show the presence of lines due to Ar^* and H^* species.⁴⁰ Partially decomposed species of the precursor molecule of the type TiO_xCy would interact very weakly with the growing surface of the film and could diffuse onto it until they become oxidized by oxygen species coming from the plasma. Only when this occurs, titanium would remain anchored onto the surface by formation of direct Ti-O-Ti_(surf) bonds.

The different microstructures and porosities of these two types of TiO_2 films prepared in this work are congruent with this picture of the growing processes. According to that, a high sticking coefficient and a low mobility of the *ad-species* yield a columnar growth as it is effectively found for the samples prepared with 100% O_2 plasma. The porosity of this columnar microstructure consists of micro- and meso-pores.

We think that it is possible to associate the mesopores with the empty space remaining between the columns. For the O_2+Ar plasma, surface diffusion of the *ad-species* and the lateral growth of the surface grains due to the off-perpendicular arrival of plasma species²⁴ prevent the formation of columns. Growth of the films occurs by coalescence of very small grains growing laterally. Although the microstructure of these samples is characterized by a homogeneous aspect, they contain a high volume of micropores. According to the above considerations about the growing process of these thin films, the micropores in these samples would correspond to the interparticular space remaining after coalescence of grains.

IV. CONCLUDING REMARKS

The present paper tries to describe the growth mechanism of TiO_2 thin films prepared by plasma deposition through the analysis of their scaling behavior. The analysis of the scaling parameters α and β has provided some clues to realize the importance of factors like shadowing, surface diffusion, or lateral growth in the surface growth mechanism of the films. Depending on the plasma conditions, these processes are more or less favored, thus leading to films with quite different microstructures and porosities. An additional aspect is the attempt to correlate the scaling behavior of the films with their porosity and microstructure.

The work presents a methodology to determine the porosity of thin films consisting of the implementation in this field of the classical adsorption methods utilized for characterization of powder materials. In particular, by using the t-plots of the water adsorption isotherms it has been proved that thin films with a similar overall porosity may present either mi-

crospores or a mixture of micro- and meso-pores, depending on the preparation conditions.

By means of the analysis of the scaling behavior of the thin films, the microporosity has been associated with a growing mechanism where surface diffusion and lateral growth are the key factors that control the film growth. By contrast, the development of mesoporosity and a columnar microstructure have been associated with a growing mechanism where the plasma species present a high sticking coefficient and hence low surface diffusivity. In this case shadowing effects are critical for the control of the final microstructure. Since, except for the type of chemistry in the plasma, all other deposition conditions were similar for the two kinds of thin films, it is proposed that plasma chemistry is a key factor to explain the found differences. In this context it is worthy of note that control of microstructure by other techniques like physical vapor deposition requires the intervention of other process parameters like temperature of substrate or pressure during deposition.⁴²

Finally, from the point of view of the optical application of the films it is interesting to remark the finding that the adsorption of water in mesoporous films may present hysteresis and be partially irreversible, while in microporous films total reversibility occurs. Due to the change in refraction index due to the water adsorption in the pores, these two different behaviors are relevant when the thin films are to be used for optical applications under real conditions of work and, particularly, if the humidity of the environment may change during time.^{43,44}

ACKNOWLEDGMENTS

We thank the Spanish Ministry of Science and Education for financial support (Grants No. NAN2004-09317-C04-01 and No. MAT2007-65764).

-
- ¹D. Mergel, D. Buschendorf, S. Eggert, R. Grammes, and B. Samset, *Thin Solid Films* **371**, 218 (2000).
²A. Brunet-Bruneau, S. Fisson, B. Gallas, G. Vuye, and J. Rivory, *Thin Solid Films* **377**, 57 (2000).
³R. E. Klinger and C. K. Carniglia, *Appl. Opt.* **24**, 3184 (1985).
⁴H. J. Cho and Ch. K. Hwangbo, *Appl. Opt.* **35**, 5545 (1996).
⁵M. Montecchi, *Pure Appl. Opt.* **4**, 831 (1995).
⁶Md. Mosaddeq-ur-Rahman, G. Yu, T. Soga, T. Jimbo, H. Ebisu, and M. Umeno, *J. Appl. Phys.* **88**, 4634 (2000).
⁷Y. Leprince-Wang, K. Yu-Zhang, V. Nguyen Van, D. Souche, and J. Rivory, *Thin Solid Films* **38**, 307 (1997).
⁸A. Egio, P. Fernández, O. Conde, and T. Vilajuana, *Proceedings of the 19th Congress of the International Commission for Optics*, edited by A. Consortini and G. C. Righini, SPIE Proceedings Series, International Society for Optical Engineering, (Bellingham, WA, 2002), Vol. 4829, p. 743.
⁹A. Amassian, P. Desjardins, and L. Martinu, *Thin Solid Films* **447**, 40 (2004).
¹⁰G. A. Battiston, R. Gerbasi, A. Gregori, M. Porchia, S. Cattarin, and G. A. Rizzi, *Thin Solid Films* **371**, 126 (2000).
¹¹F. Gracia, J. P. Holgado, and A. R. González-Elipe, *Langmuir* **20**, 1688 (2004).
¹²L. Martinu and D. Poitras, *J. Vac. Sci. Technol. A* **18**, 2619 (2000).
¹³K. Ostrikov, *Rev. Mod. Phys.* **77**, 489 (2005).
¹⁴T. Busani and R. A. B. Devine, *Semicond. Sci. Technol.* **20**, 870 (2005).
¹⁵S. Pongratz and A. Zoller, *Annu. Rev. Mater. Sci.* **22**, 279 (1992).
¹⁶A.-L. Barabasi and H. E. Stanley, *Fractal Concepts in Surface Growth* (Cambridge University Press, Cambridge, England, 1994).
¹⁷S. J. Fang, *J. Appl. Phys.* **82**, 5891 (1997).
¹⁸S. G. Mayr, M. Moske, and K. Samwer, *Phys. Rev. B* **60**, 16950 (1999).
¹⁹F. Elsholtz, E. Scholl, and A. Rosenfeld, *Appl. Phys. Lett.* **84**, 4167 (2004).
²⁰G. T. Dalakos, J. P. Plawsky, and P. D. Persans, *Phys. Rev. B* **72**, 205305 (2005).
²¹I.-Y. Kim, S.-H. Hong, A. Consoli, J. Benedikt, and A. von Keudell, *J. Appl. Phys.* **100**, 053302 (2006).
²²J. M. Lopez, M. Castro, and R. Gallego, *Phys. Rev. Lett.* **94**, 166103 (2005).

- ²³S. Huo and W. Schwarzacher, *Phys. Rev. Lett.* **86**, 256 (2001).
- ²⁴A. Yanguas-Gil, J. Cotrino, A. Barranco, and A. R. González-Elipe, *Phys. Rev. Lett.* **96**, 236101 (2006).
- ²⁵S. J. Gregg and K. S. W. Sing, *Adsorption, Surface Area and Porosity* (Academic Press, London, 1982).
- ²⁶A. Bourgeois, A. Brunet-Bruneau, V. Jousseume, N. Rochat, S. Fisson, B. Demarets, and J. Rivory, *Thin Solid Films* **455**, 366 (2004).
- ²⁷A. Alvarez-Herrero, H. Guerrero, E. Bernabeu, and D. Levy, *Appl. Opt.* **41**, 6692 (2002).
- ²⁸M. R. Baklanov, K. P. Mogilnikov, V. G. Polovinkin, and F. N. Dultsev, *J. Vac. Sci. Technol. B* **18**, 1385 (2000).
- ²⁹F. N. Dultsev and M. R. Baklanov, *Electrochem. Solid-State Lett.* **24**, 192 (1999).
- ³⁰A. Ruud Balkenende, F. K. de Theije, and J. C. Koen Kriege, *Adv. Mater. (Weinheim, Ger.)* **15**, 139 (2003).
- ³¹V. Rouessac, R. Coustel, F. Bosc, J. Durand, and A. Ayrat, *Thin Solid Films* **495**, 232 (2006).
- ³²A. Barranco, J. Cotrino, F. Yubero, J. P. Espinós, J. Benítez, C. Clero, and A. R. González-Elipe, *Thin Solid Films* **401**, 150 (2001).
- ³³*Handbook of Chemistry and Physics*, 78th ed., edited by D. R. Lide (CRC, New York, 1997).
- ³⁴M. Kondo, T. Ohe, K. Saito, T. Nishimiya, and A. Matsuda, *J. Non-Cryst. Solids* **890**, 227 (1998).
- ³⁵F. Ojeda, R. Cuerno, R. Salvarezza, and L. Vázquez, *Phys. Rev. Lett.* **84**, 3125 (2000).
- ³⁶M. Kardar, G. Parisi, and Y.-C. Zhang, *Phys. Rev. Lett.* **56**, 889 (1986).
- ³⁷Z. W. Lai and S. Das Sarma, *Phys. Rev. Lett.* **66**, 2348 (1991).
- ³⁸D. E. Wolf and J. Vilain, *Europhys. Lett.* **13**, 389 (1990).
- ³⁹A. E. Lita and J. E. Sánchez, *Phys. Rev. B* **61**, 7692 (2000).
- ⁴⁰A. Borrás, Á. Barranco, J. P. Espinós, J. Cotrino, J. P. Holgado, and A. R. González-Elipe, *Plasma Processes Polym.* **4**, 515 (2007).
- ⁴¹M. Nakamura, S. Kato, T. Aoki, L. Sirghi, and Y. Hatanaka, *Thin Solid Films* **401**, 138 (2001).
- ⁴²J. A. Thornton, *Annu. Rev. Mater. Sci.* **7**, 239 (1977).
- ⁴³A. Priyadarshi, L. Shimin, E. H. Wong, R. Rajoo, S. G. Mhaisalkar, and V. Kripesh, *J. Electron. Mater.* **34**, 1378 (2005).
- ⁴⁴A. Alvarez-Herrero, G. Ramos, E. del Monte, E. Bernabeu, and D. Levy, *Thin Solid Films* **455**, 356 (2004).